JOC The Journal of Organic Chemistry

Note

pubs.acs.org/joc

Three Rhodamine-Based "Off–On" Chemosensors with High Selectivity and Sensitivity for Fe^{3+} Imaging in Living Cells

Zheng Yang,[†] Mengyao She,[†] Bing Yin,[†] Jihong Cui,[‡] Yuze Zhang,[†] Wei Sun,[†] Jianli Li,*[,†] and Zhen Shi[†]

[†]Ministry of Education Key Laboratory of Synthetic and Natural Functional Molecule Chemistry, College of Chemistry & Materials Science, Northwest University, Xi'an, Shaanxi 710069, PR China

[‡]College of Life Sciences, Northwest University, Xi'an, Shaanxi 710069, PR China

Supporting Information

ABSTRACT: Three new rhodamine-based probes **Y1**–**Y3** were synthesized as "off–on" chemosensors for Fe^{3+} imaging in living cells. The recognizing behaviors were investigated both experimentally and computationally. The crystal structure of the complex **Y3**-Fe^{3+} revealed that Fe^{3+} preferred to coordinate with the N atom of benzothiazole moiety rather than the O atom of carboxyl group.

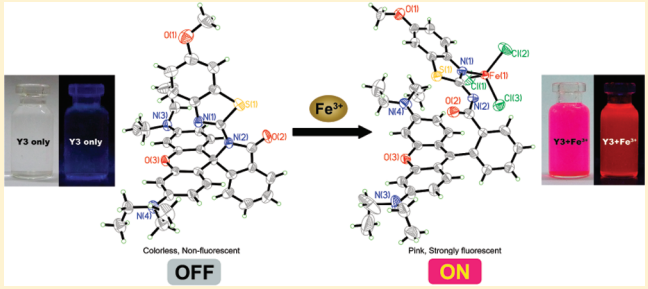

The design and synthesis of highly selective and sensitive chemosensors for biologically and environmentally important ionic species have attracted a great deal of attention.[1] As one of the most essential trace elements in biological systems, Fe^{3+} performs a major role in many biochemical processes at the cellular level.[2] High levels of Fe^{3+} within the body have been associated with increasing incidence of certain cancers and dysfunction of certain organs, such as the heart, pancreas, and liver.[3] Recent research suggests that Fe^{3+} could also be involved in the underlying mechanisms of many neurodegenerative diseases, such as Parkinson's disease and Alzheimer's disease.[4] Therefore, a convenient and rapid method for the analysis of Fe^{3+} in biological samples has important consequences in biological and environmental concerns. Considerable efforts have been devoted to the development of Fe^{3+}-selective sensors. Unfortunately, there have been relatively few fluorescent chemosensors for Fe^{3+} because of the fluorescent quenching of the paramagnetic nature of Fe^{3+}.[5] Recently, Lee et al.[6] developed a Fe^{3+}-selective sensor that could demonstrate sensitive and selective detection of intracellular Fe^{3+} in hepatocytes. At present, the research works related to this area are of great challenge and interest.

On the other hand, fluorescent signaling has been widely used in environmental and biological science,[7] among which rhodamine dyes appear to be particularly attractive for the construction of an "off-on" type fluorescent chemosensor,[8] owing to their simplicity, low detection limit, the capability for special recognition and excellent spectroscopic properties.[9] Recently, on the basis of spirolactam to ring-open amide equilibrium of rhodamine, a number of rhodamine dyes have been utilized for the detection of metal ions, such as Cu^{2+}, Hg^{2+}, Cr^{3+}, Pb^{2+}, and Au^{+}.[10]

With the above-mentioned criteria in mind, herein we introduced benzothiazole moieties to rhodamine and got three probes, **Y1**, **Y2**, and **Y3** (Scheme 1), which can give highly selective and rapid responses to Fe^{3+} in living cells. Although **Y1**–**Y3** exhibited different fluorescence intensities when binding with 1.0 equiv of Fe^{3+}, the emission wavelengths of each probes appeared at 580 nm. Good linear relationships were observed between the relative fluorescence intensities of the probes and the concentration of Fe^{3+} in the 5–20 μM range with a detection limit of 5 μM. The results suggested that the R moiety had no significant effect on the spectral properties of the probes. Thus, only compound **Y3** was chosen for the following discussion; optical spectra of **Y1** and **Y2** are shown in the Supporting Information (Figures S2–S11). The molecular structure of **Y3** is shown in Figure 1a.

Absorption and fluorescence titrations of **Y3** were conducted in methanol–water (4.5/5.5, v/v) solution (Figure 2). As expected, no obvious absorption and fluorescent emission were observed in the absence of Fe^{3+} because the spirocyclic form of rhodamine prevailed. However, upon treating with Fe^{3+}, an intense absorption band centered at 558 nm, and concomitantly, a strong orange fluorescent emission band appeared at 580 nm, which was reasonably assigned to the delocalized xanthene tautomer of the rhodamine group. The titration curve showed a steady and smooth increase, and about 1.0 equiv of Fe^{3+} was required until a plateau was reached (Figure 2a, inset) with the quantum yield[11] as 0.34. Job's plot showed a 1:1 stoichiometry between **Y3** and Fe^{3+} (Figure 2b, inset). The association constant was estimated to be 4.52×10^5 M^{-1}.[12] Addition of ethylenediamine to the mixture of **Y3** (20 μM) and Fe^{3+} (20 μM) decreased the color and fluorescence intensity of

Received: October 10, 2011
Published: December 17, 2011

dx.doi.org/10.1021/jo202056t | J. Org. Chem. 2012, 77, 1143–1147

Scheme 1. Synthesis of Y1, Y2, and Y3

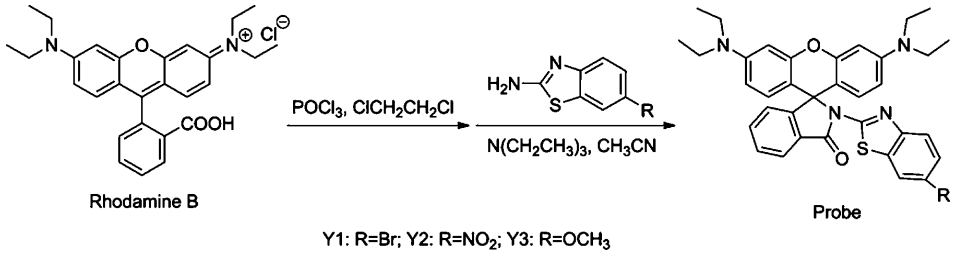

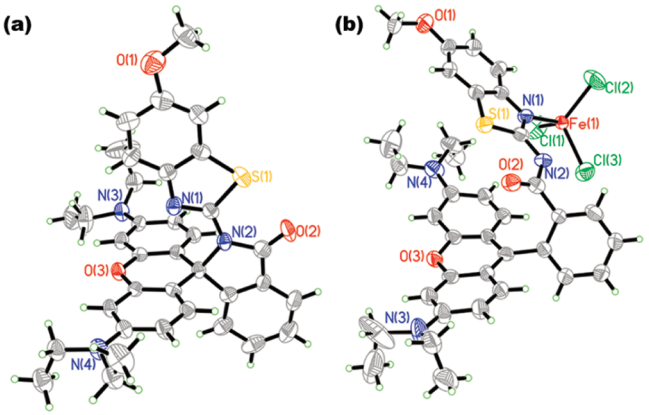

Figure 1. Molecular structures of **Y3** (a) and **Y3**-Fe^{3+} (b).

the solution (Figure S12, Supporting Information), which implied the reversible binding between **Y3** and Fe^{3+}.

Related heavy, transition, and main group metal ions, including Li^+, Na^+, K^+, Ba^{2+}, Ca^{2+}, Cd^{2+}, Mg^{2+}, Co^{2+}, Mn^{2+}, Zn^{2+}, Pb^{2+}, Ni^{2+}, Hg^{2+}, Ag^+, Cr^{3+}, Cu^{2+}, and Fe^{2+} together with Fe^{3+}, were used to evaluate the selectivity of **Y3** in methanol–water (4.5/5.5, v/v) solution. As shown in Figure 3, only the addition of Fe^{3+} resulted in a prominent enhancement of fluorescence at 580 nm (absorbance at 558 nm), which obviously implied the high selectivity of **Y3** to Fe^{3+}. The competition experiments, which were carried out by adding Fe^{3+} to **Y3** solution in the presence of other metal ions, revealed that the Fe^{3+}-induced fluorescent responses were not significantly interfered by the commonly coexistent metal ions (Figure S12, Supporting Information).

In order to gain insight into the ring-opening mechanism, 1.0 equiv of $FeCl_3$ was conducted with each probe in CH_3CN/CH_3OH. Delightfully, the single crystal of **Y3**-Fe^{3+} was obtained (Figure 1b). Surprisingly, coordination of Fe^{3+} selectively occurred at the N atom on the benzothiazole ring rather than the O atom[13] of the carbonyl moiety.

IR spectra of **Y3** and **Y3**-Fe^{3+} were then measured to confirm the binding mechanism. The peak at 1702 cm^{-1}, corresponding to the characteristic carbonyl absorption of **Y3**, did not drastically shift to the lower frequency upon addition of 1.0 equiv of Fe^{3+} (Figure S16, Supporting Information). This supported that the amide carbonyl oxygen is actually not involved in the coordination.

For better understanding, theoretical calculations of **Y3** and **Y3**-Fe^{3+} complex were performed at DFT level with B3LYP[14] functional. The optimized geometries of **Y3** and **Y3**-Fe^{3+} complex are shown in Figure S15 (Supporting Information), of which the local minimum character was confirmed by the nonexistence of imaginary frequency. The spatial distributions and orbital energies of HOMO and LUMO of **Y3**-Fe^{3+} were also determined (Figure 4).

In the case of previous works, coordination of carbonyl oxygen to metal ions led to spirocycle opening,[13] whereas in this study, it was clearly shown that Fe^{3+} was coordinated with the N atom of the benzothiazole moiety rather than the carbonyl O atom. The priority of the N atom over the O atom

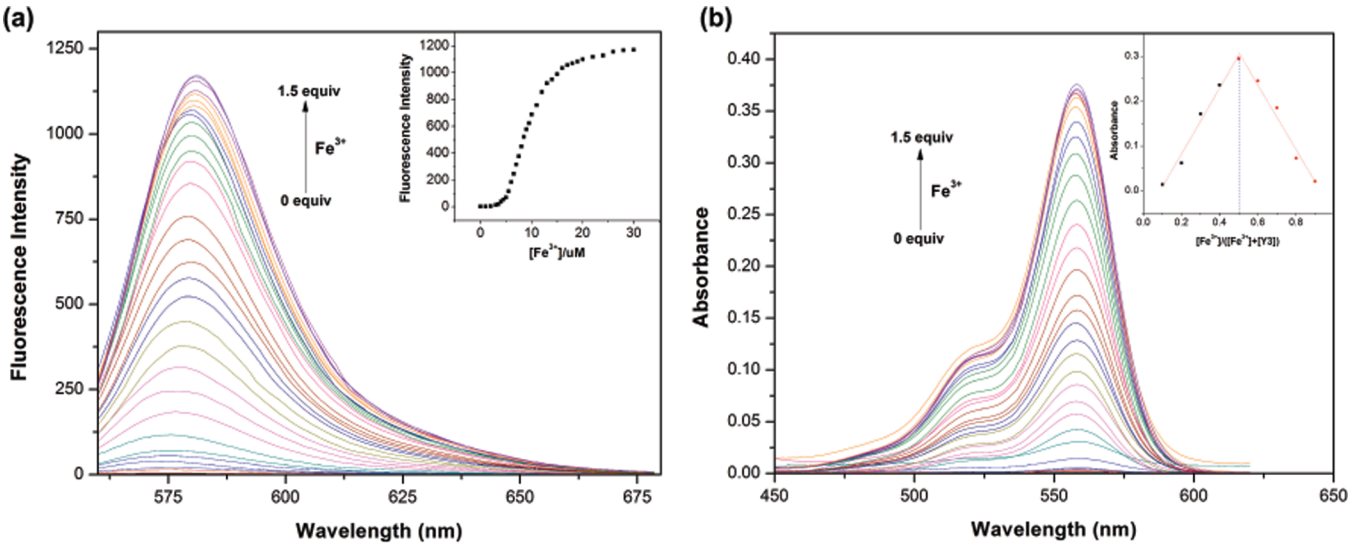

Figure 2. Fluorescence intensity (a) and absorption (b) changes of **Y3** (20 μM) upon addition of Fe^{3+} (0–1.5 equiv) in methanol–water (4.5/5.5, v/v) solution. Inset: (a) Changes of emission intensity at 580 nm. λ_{ex} = 550 nm. (b) Job's plot of **Y3** and Fe^{3+}.

dx.doi.org/10.1021/jo202056t | J. Org. Chem. 2012, 77, 1143–1147

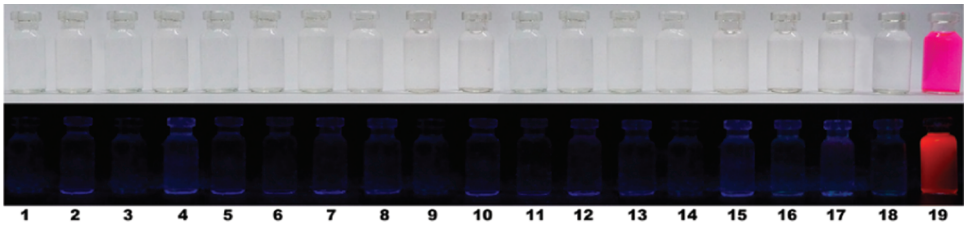

Figure 3. Color and fluorescent changes of **Y3** (20 μM) upon the addition of various metal ions (20 μM). 1, blank; 2, Li^{+}; 3, Na^{+}; 4, K^{+}; 5, Ba^{2+}; 6, Ca^{2+}; 7, Cd^{2+}; 8, Ag^{+}; 9, Mg^{2+}; 10, Co^{2+}; 11, Mn^{2+}; 12, Zn^{2+}; 13, Pb^{2+}; 14, Hg^{2+}; 15, Ni^{2+}; 16, Cr^{3+}; 17, Cu^{2+}; 18, Fe^{2+}; 19, Fe^{3+}.

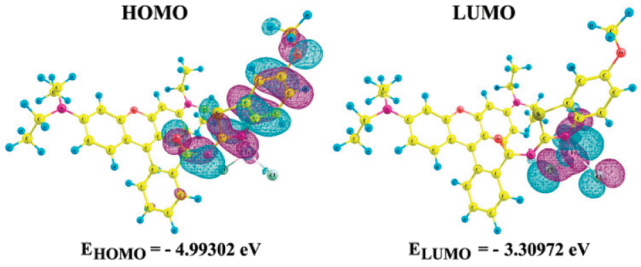

Figure 4. HOMO and LUMO distributions of **Y3**-Fe^{3+}.

in coordination with Fe^{3+} may be explained on the basis of the NBO analysis[15] of the lone pair (LP) orbitals of N and O atoms in the probe **Y3**. The spatial extent of the LP of the N atom was shown to be larger than that of the O atom and thus facilitates its contact with Fe^{3+}. In energetic terms, the orbital energy of the LP of the N atom was significantly higher than that of the O atom. Therefore, compared with the O atom, the coordination of the Fe^{3+} to the N atom should be more energetically favorable. Thus, it can be supposed that Fe^{3+} prefers to coordinate with the N atom of the benzothiazole moiety accompanied by the transferring of electrons forming the quinoid structure, which resulted in the changes in fluorescence (Scheme 2).

Practical bioimaging applications of the probes for Fe^{3+} in Hela cells were developed by laser scanning confocal microscopy. Cultured Hela cells were incubated with the probes in culture medium for 30 min at 37 °C, and very weak intracellular fluorescence inside the living Hela cells were observed (Figure 5a). The cells were supplemented with 20 μM $FeCl_3$ in the growth medium for 30 min at 37 °C and then loaded with the probes under the same condition, whereupon a significant increase in the fluorescence from the intracellular area was observed (Figure 5b). Bright-field transmission images of cells treated with the probes and Fe^{3+} confirmed that the cells were viable throughout the imaging experiments (Figure 5c). As depicted in Figure 5d, the overlay of fluorescence and bright-field images revealed that the fluorescence signals were localized in the perinuclear area of the cytosol, indicating a subcellular distribution of Fe^{3+}. The results indicated that the probes could respond to the changes of the concentration of Fe^{3+} in living cells.

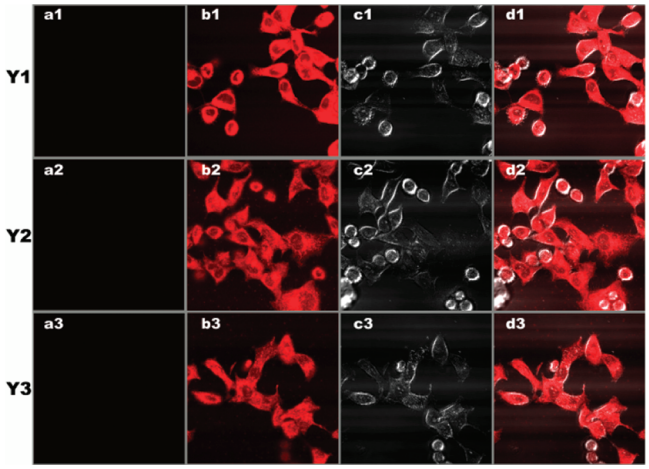

Figure 5. Fluorescent images of Hela cells incubated with 20 μM probes for 30 min (a) and then further incubated with 20 μM Fe^{3+} for 30 min (b). (c) Cells supplemented with 20 μM probes in the growth media for 30 min at 37 °C and then incubated with 20 μM Fe^{3+} for 30 min at 37 °C. The overlay image of (b) and (c) is shown in (d) (λ_{ex} = 543 nm).

In conclusion, three rhodamine-based highly sensitive and selective chemosensors have been developed for the detection of Fe^{3+}. Both the single crystal structure of the **Y3**-Fe^{3+} complex and the theoretical studies supported that Fe^{3+} coordinating with the N atom of the benzothiazole moiety, accompanied by the transferring of electrons of the benzothiazole, resulted in the opening of the spiro-ring. Confocal laser scanning microscopy experiments have proven that the probes can be used to monitor Fe^{3+} in living cells.

EXPERIMENTAL SECTION

General Methods. Fe^{3+} stock solution (5.00 mM): In a 25 mL volumetric flask, 20.27 mg of anhydrous $FeCl_3$ was dissolved in water and then diluted to the mark with water. The other metal ions were prepared as 5.00 mM in water. The solutions of metal ions were performed from their nitrate and chloride salts.

Scheme 2. Proposed Mechanism for the Fluorescent Changes of Y3 upon the Addition of Fe^{3+}

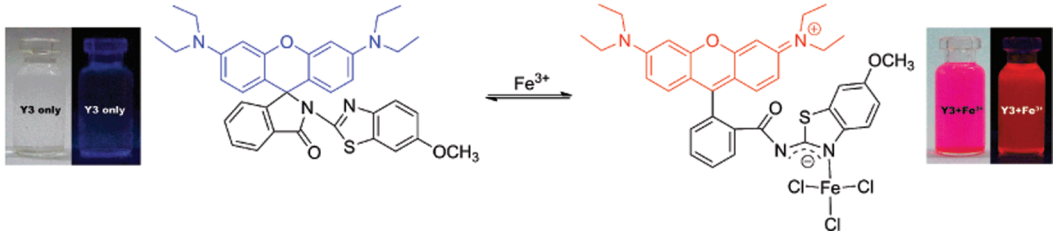

dx.doi.org/10.1021/jo202056t | J. Org. Chem. 2012, 77, 1143–1147

Rhodamine-B-based probes stock solution (200 μM): In a 25 mL volumetric flask, 0.0625 mmol sensors (**Y1**: 0.04084 g, **Y2**: 0.03873 g, **Y3**: 0.03780 g) were dissolved in acetone and then diluted to the mark with acetone. To a 50 mL volumetric tube, 4.00 mL of the solution was added and diluted to 50 mL with methanol.

For colorimetric determination of Fe^{3+}, 1.00 mL of 200 μM probes and different concentrations of Fe^{3+} were added to a 10 mL volumetric tube, 3.5 mL of methanol was added, and the mixture was diluted to the mark with water. Then, the absorbance was recorded at 558 nm. The fluorescence intensity of the above solutions was recorded at 580 nm with excitation wavelength set at 550 nm. The excitation and emission wavelength bandpasses were both set at 5.0 nm.

Synthesis of Compounds Y1−Y3. In brief, to a stirred solution of rhodamine hydrochloride (4.78 g, 0.01 mol) and 2-dichloroethane (10 mL), 5 mL of phosphorus oxychloride was added. The solution was refluxed for 6 h and concentrated by evaporation. The obtained crude acid chloride was dissolved in acetonitrile (10 mL). Then, a solution of the benzothiazole derivatives (0.01 mol) and triethylamine (5 mL) in acetonitrile (20 mL) was added dropwise in 30 min. After refluxing for 4 h, the solvent was removed under reduced pressure to give a violet oil. Water was then added to the mixture, and the aqueous phase was extracted with dichloromethane (15 mL × 3). The organic layer was washed with water, dried over anhydrous $MgSO_4$, and filtered. Purification of the products was by column chromatography on silica gel (eluant: CH_2Cl_2).

Compound **Y1**: Yellow powder, 2.68 g; yield 41%; mp 235−236 °C; ^{1}H NMR ($CDCl_3$, 400 MHz, TMS) δ (ppm) 8.06 (d, J = 7.3 Hz, 1H), 7.80 (d, J = 1.5 Hz, 1H), 7.58 (dt, J_1 = 20.7, J_2 = 7.3 Hz, 2H), 7.47 (d, J = 8.6 Hz, 1H), 7.34 (dd, J_1 = 8.6, J_2 = 1.7 Hz, 1H), 7.28−7.16 (m, 1H), 6.54−6.26 (m, 4H), 6.13 (dd, J_1 = 8.8, J_2 = 2.4 Hz, 2H), 3.29 (q, J = 8.0 Hz, 8H), 1.12 (t, J = 7.0 Hz, 12H); ^{13}C NMR ($CDCl_3$, 100 MHz, TMS) δ (ppm) 167.0, 154.3, 153.5, 148.9, 148.7, 134.6, 134.0, 123.0, 128.4, 128.0, 124.9, 123.5, 123.2, 116.1, 107.1, 106.1, 97.4, 68.4, 44.3, 12.6. Anal. Calcd for $C_{35}H_{33}BrN_4O_2S$: H, 5.09; C, 64.31; N, 8.57; S, 4.91. Found: H, 5.08; C, 64.50; N, 8.60; S, 4.90.

Compound **Y2**: Yellow powder, 4.22 g; yield 68%; mp 209−210 °C; ^{1}H NMR ($CDCl_3$, 400 MHz, TMS) δ (ppm) 8.63 (s, 1H), 8.12 (dd, J_1 = 20.3, J_2 = 8.2 Hz, 2H), 7.83−7.41 (m, 4H), 7.27 (d, J = 4.8 Hz, 2H), 6.46 (d, J = 1.4 Hz, 1H), 6.39 (d, J = 8.8 Hz, 1H), 6.24−6.06 (m, 2H), 3.29 (q, J = 6.8 Hz, 8H), 1.14 (t, J = 6.9 Hz, 12H); ^{13}C NMR ($CDCl_3$, 100 MHz, TMS) δ (ppm) 167.3, 158.5, 154.4, 154.1, 153.3, 148.9, 143.2, 135.1, 132.4, 123.0, 128.6, 128.0, 125.1, 123.7, 121.6, 121.1, 117.5, 107.1, 105.7, 97.3, 68.9, 44.3, 12.6. Anal. Calcd for $C_{35}H_{33}N_5O_4S$: H, 5.37; C, 67.83; N, 11.30; S, 5.17. Found: H, 5.35; C, 67.59; N, 11.32; S, 5.18.

Compound **Y3**: Yellow powder, 3.39 g; yield 56%; mp 232−233 °C; ^{1}H NMR (400 MHz, $CDCl_3$), δ (ppm) 8.05 (d, J = 7.2 Hz, 1H), 7.72−7.41 (m, 3H), 7.32−7.07 (m, 2H), 6.87 (dd, J_1 = 8.8, J_2 = 2.4 Hz, 1H), 6.41 (dd, J_1 = 17.1, J_2 = 5.6 Hz, 4H), 6.13 (dd, J_1 = 8.8, J_2 = 2.4 Hz, 2H), 3.79 (s, 3H), 3.29 (q, J = 4.0 Hz, 6.4H), 1.13 (t, J = 7.0 Hz, 12H); ^{13}C NMR (100 MHz, $CDCl_3$), δ (ppm) 166.8, 156.4, 154.4, 153.6, 152.1, 148.9, 144.1, 134.3, 133.4, 129.3, 128.6, 128.0, 124.9, 123.4, 122.6, 114.2, 107.2, 106.5, 103.8, 97.6, 68.1, 55.9, 44.3, 12.7. Anal. Calcd for $C_{36}H_{36}N_4O_3S$: H, 6.00; C, 71.50; N, 9.26; S, 5.30. Found: H, 5.99; C, 71.39; N, 9.29; S, 5.32.

■ ASSOCIATED CONTENT

Supporting Information

Experimental data, synthetic details, copies of IR, ^{1}H NMR, ^{13}C NMR, and optical spectra, and other data. This material is available free of charge via the Internet at http://pubs.acs.org.

■ AUTHOR INFORMATION

Corresponding Author

*Tel.: +86 029 88302604. Fax: +86 029 88302601. E-mail: lijianli@nwu.edu.cn.

■ ACKNOWLEDGMENTS

The project was supported by National Natural Science Foundation of China (No. 20972124), the China Postdoctoral Science Foundation (No. 20080441180), the Chinese National Science Foundation for Talent Training (No. J0830417), and Chinese National Innovation Experiment Program for University Students (No. 101069702). Y.B. wants to express his thanks to Prof. Yuanhe Huang (College of Chemistry, Beijing Normal University) for his great help.

■ REFERENCES

(1) (a) Dujols, V.; Ford, F.; Czarnik, A. W. *J. Am. Chem. Soc.* **1997**, *119*, 7386−7187. (b) Martinez-Manez, R.; Sancenon, F. *Chem. Rev.* **2003**, *103*, 4419−4476. (c) Gunnlaugsson, T.; Glynn, M.; Tocci, G. M.; Kruger, P. E.; Pfeffer, F. M. *Coord. Chem. Rev.* **2006**, *250*, 3094−3117. (d) Kim, J. S.; Quang, D. T. *Chem. Rev.* **2007**, *107*, 3780−3799. (e) Kim, H. N.; Lee, M. H.; Kim, H. J.; Kim, J. S.; Yoon, J. *Chem. Soc. Rev.* **2008**, *37*, 1465−1472.

(2) (a) D'Autreaux, B.; Tucker, N. P.; Dixon, R.; Spiro, S. *Nature* **2005**, *437*, 769−772. (b) Lee, J. W.; Helmann, J. D. *Nature* **2006**, *440*, 363−367. (c) Weizman, H.; Ardon, O.; Mester, B.; Libman, J.; Dwir, O.; Hadar, Y.; Chen, Y.; Shanzer, A. *J. Am. Chem. Soc.* **1996**, *118*, 12368−12375. (d) Sumner, J. P.; Kopelman, R. *Analyst* **2005**, *130*, 528−533.

(3) (a) Halliwell, B. *J. Neurochem.* **1992**, *59*, 1609−1623. (b) Weinberg, E. D. *Eur. J. Cancer Prev.* **1996**, *5*, 19−36. (c) Galaris, D.; Skiada, V.; Barbouti, A. *Cancer Lett.* **2008**, *266*, 21−29.

(4) (a) Crichton, R. R.; Dexter, D. T.; Ward, R. J. *Coord. Chem. Rev.* **2008**, *252*, 1189−1199. (b) Dornelles, A. S.; Garcia, V. A.; de Lima, M. N.; Vedana, G.; Alcalde, L. A.; Bogo, M. R.; Schroeder, N. *Neurochem. Res.* **2010**, *35*, 564−571.

(5) (a) Bricks, J. L.; Kovalchuk, A.; Trieflinger, C.; Nofz, M.; Bueschel, M.; Tolmachev, I.; Daub, J.; Rurack, K. *J. Am. Chem. Soc.* **2005**, *127*, 13522−13529. (b) Xiang, Y.; Tong, A. J. *Org. Lett.* **2006**, *8*, 1549−1552. (c) Zhang, X.; Shiraishi, Y.; Hirai, T. *Tetrahedron Lett.* **2007**, *48*, 5455−5459. (d) Dong, L.; Wu, C.; Zeng, X.; Mu, L.; Xue, S. F.; Tao, Z.; Zhang, J. X. *Sens. Actuators, B* **2010**, *B145*, 433−437. (e) Wang, B. D.; Hai, J.; Liu, Z. C.; Wang, Q.; Yang, Z. Y; Sun, S. H. *Angew. Chem., Int. Ed.* **2010**, *49*, 4576−4579.

(6) Lee, M. H.; Giap, T. V.; Kim, S. H.; Lee, Y. H.; Kang, C.; Kim, J. S. *Chem. Commun.* **2010**, *46*, 1407−1409.

(7) (a) Malashikhin, S.; Finney, N. S. *J. Am. Chem. Soc.* **2008**, *130*, 12846−12847. (b) Ostergaard, M. E.; Cheguru, P.; Papasani, M. R.; Hill, R. A.; Hrdlicka, P. J. *J. Am. Chem. Soc.* **2010**, *132*, 14221−14228. (c) Tan, S. S.; Kim, S. J.; Kool, E. T. *J. Am. Chem. Soc.* **2011**, *133*, 2664−2671.

(8) (a) Pires, M. M.; Chmielewski, J. *Org. Lett.* **2008**, *10*, 837−840. (b) Kou, S.; Lee, H. N.; van Noort, D.; Swamy, K. M.; Kim, S. H.; Soh, J. H.; Lee, K.; Nam, S. W.; Yoon, J.; Park, S. *Angew. Chem., Int. Ed.* **2008**, *47*, 872−876. (c) Zhang, J. F.; Zhou, Y.; Yoon, J.; Kim, Y.; Kim, S. J.; Kim, J. S. *Org. Lett.* **2010**, *12*, 3853−3855.

(9) Ramette, R. W.; Sandell, E. B. *J. Am. Chem. Soc.* **1956**, *78*, 4872−4878.

(10) (a) Royzen, M.; Dai, Z. H.; Canary, J. W. *J. Am. Chem. Soc.* **2005**, *127*, 1612−1613. (b) Shiraishi, Y.; Sumiya, S.; Kohno, Y.; Hirai, T. *J. Org. Chem.* **2008**, *73*, 8571−8574. (c) Huang, K. W.; Yang, H.; Zhou, Z. G.; Yu, M. X.; Li, F. Y.; Gao, X.; Yi, T.; Huang, C. H. *Org. Lett.* **2008**, *10*, 2557−2560. (d) Kwon, J. Y.; Jang, Y. J.; Lee, Y. J.; Kim, K. M.; Seo, M. S.; Nam, W.; Yoon, J. *J. Am. Chem. Soc.* **2005**, *127*, 10107−10111. (e) Yang, Y.; Lee, S.; Tae, J. *Org. Lett.* **2009**, *11*, 5610−5613.

(11) Huang, W.; Song, C. X.; He, C.; Lv, G. J.; Hu, X. Y.; Zhu, X.; Duan, C. Y. *Inorg. Chem.* **2009**, *48*, 5061−5072.

(12) (a) Bourson, J.; Pouget, J.; Valeur, B. *J. Phys. Chem.* **1993**, *97*, 4552−4557. (b) Zhao, Y.; Zhang, X. B.; Han, Z. X.; Qiao, L.; Li, C. Y.; Jian, L. X.; Shen, G. L.; Yu, R. Q. *Anal. Chem.* **2009**, *81*, 7022−7030.

(13) (a) Wu, D. Y.; Huang, W.; Duan, C. Y.; Lin, Z. H.; Meng, Q. J. *Inorg. Chem.* **2007**, *46*, 1538−1540. (b) Huang, W.; Zhu, X.; Wua, D. Y.; He, C.; Hu, X. Y.; Duan, C. Y. *Dalton Trans.* **2009**, 10457−10465.
(14) (a) Becke, A. D. *J. Chem. Phys.* **1993**, *98*, 5648−5652. (b) Lee, C.; Yang, W.; Parr, R. G. *Phys. Rev. B: Condens. Matter Mater. Phys.* **1988**, *37*, 785−789.
(15) (a) Reed, A. E.; Curtiss, L. A.; Weinhold, F. *Chem. Rev.* **1988**, *88*, 899−926. (b) Yin, B.; Huang, Y. H.; Wang, G.; Wang, Y. *J. Mol. Model.* **2010**, *16*, 437−446.

dx.doi.org/10.1021/jo202056t | *J. Org. Chem.* 2012, 77, 1143−1147